ISSN 1063-7834, Physics of the Solid State, 2017, Vol. 59, No. 2, pp. 304–309. © Pleiades Publishing, Ltd., 2017.
Original Russian Text © A.V. Golenishchev-Kutuzov, V.A. Golenishchev-Kutuzov, R.I. Kalimullin, A.V. Semennikov, 2017, published in Fizika Tverdogo Tela, 2017, Vol. 59, No. 2, pp. 296–301.

FERROELECTRICITY

Dynamics of Photo-Induced Changes in the Elastic Characteristics of Lithium Niobate Crystals Doped with Jahn–Teller Fe^{2+} Ions

A. V. Golenishchev-Kutuzov, V. A. Golenishchev-Kutuzov, R. I. Kalimullin, and A. V. Semennikov

Kazan State Power Engineering University, ul. Krasnosel'skaya 51, Kazan, Tatarstan, 420066 Russia

e-mail: campoce6e@gmail.com

Received July 18, 2016

Abstract—The effect of admixture Jahn–Teller Fe^{2+} ions on the elastic characteristics of lithium niobate was studied. The appearance of photostrains and a change in elastic moduli under the influence of laser radiation was established, thus enabling the creation of device elements with optically controlled elastic characteristics.

DOI: 10.1134/S106378341702007X

1. INTRODUCTION

Lithium niobate crystals ($LiNbO_3$-LN), both pure and doped with ions of transition groups, have been used in acousto- and optoelectronic instruments for many decades [1–3]. Their application has considerably grown as late as in the XXI century due to the development of new methods for the formation of periodic domain structures with micro- and then nanosized periods [4–6]. In all the past years, much attention was paid to unordinary great nonlinear optical and photo-induced effects, but some changes in the velocity of acoustic waves in an applied electrical field [7, 8] and under the influence of laser radiation [9–11] have been revealed as far back as in the 1970–1980s.

It is known that local elastic heterogeneities lead to a change in the velocity and attenuation of acoustic waves. The appearance of local elastic heterogeneities in ferropiezoelectric crystals can occur for a couple of reasons: due to the inverse piezoeffect in an electric field and microdistortions of a crystal lattice by admixture ions, which are strongly bonded to the lattice. In the works [9–11], it has been hypothesized for the first time that photo-induced changes in the elastic characteristics are associated with the presence of admixture Jahn–Teller (JT) ions in NL crystals. This hypothesis was based on the Mössbauer data [12] on studying the role of Fe^{2+} JT-ions in the physical properties of lithium niobate. Nevertheless, the later studies of photo-induced elastic strains in lithium niobate [13] relate their appearance with the inverse piezoeffect produce by the generation of a photo-induced electric field (E_{ph}). However, the photostrains $\varepsilon \sim 10^{-4}$ obtained in the work [13] by synchronous diffractometry do not correspond to photo-induced field values ($E_{ph} \sim 10^7$ V/m) attained by irradiating a LN sample containing iron ions with a xenon lamp. This circumstance does not allows us to explain the obtained results by the piezoeffect alone, though the mere fact of the influence of nearly the same concentration of Fe^{2+}, Cr^{2+}, Ni^{2+}, and V^{2+} ions on the elastic characteristics of semiconductor crystals like ZnSe was revealed in the work [14]. It is notable that the authors themselves explain the obtained results just by the JT-effect in doping ions. In some further works, the participation of admixture Fe^{2+} JT-ions [15] and structural Nb^{5+} ions (with second-order JT-effect) [16] in the formation of a number of unordinary physical characteristics of lithium niobate has also been hypothesized.

Hence, the insufficiency of notions about the nature of earlier revealed photo-induced changes in the elastic properties of doped LN crystals has given an impulse to the continuation of our studies on the role of JT-ions in the formation of the elastic properties of lithium niobate and their changes under the influence of laser radiation.

2. SAMPLES AND EXPERIMENTAL METHODS

A series of monodomenized congruent LN samples cut out in the form of rectangular X–Z section parallelepipeds with optically treated plane-parallel ends was studied. The earlier developed method of reductive (helium) and oxidative (oxygen) annealing provided the possibility to vary the concentration ratio Fe^{2+}/Fe^{3+} of doping ions from 0.1 to 0.7 (Table 1). The concentration of Fe^{2+} ions was determined from the

Table 1. Parameters of samples: dimensions, concentration ratios $C_{Fe^{2+}}/C_{Fe^{3+}}$, relative changes in velocities δV_e and attenuation $\delta\alpha$ with respect to the undoped sample depending on the concentration of iron ions and the ratio Fe^{2+}/Fe^{3+} without laser irradiation

Sample no.	Dimensions x, y, z mm	C_{Fe}, %	$C_{Fe^{2+}}/C_{Fe^{3+}}$	$\delta V_e \times 10^{-5}$	$\delta\alpha \times 10^{-5}$
1	4.5 × 5.1 × 4.0	0.01	0.3	1.6	2.0
2	4.9 × 4.5 × 4.1	0.03	0.3	5.0	6.8
3	4.7 × 5.0 × 4.1	0.05	0.3	8.1	9.2
4	4.9 × 4.5 × 4.1	0.08	0.3	11.0	11.2
5a	4.8 × 5.1 × 4.1	0.09	0.3	11.7	12.0
5b	4.8 × 5.1 × 4.1	0.09	0.1	3.8	4.1
5c	4.8 × 5.1 × 4.1	0.09	0.6	10.4	10.5

optical absorption by the method described in [17] (Table 1).

The excitation and detection of longitudinal and transverse acoustic waves within a frequency range of 150–250 MHz along axis [100] and [001] of samples were created by the natural piezoeffect using concentric or slot electrodes. The possibility to generate relatively narrow acoustic beams (~2 mm^2 or 4 × 1 mm) in combination with their scanning over different faces of samples has allowed us to perform the measurement of local elastic heterogeneities (Fig. 1). The changes in the velocity and attenuation of acoustic waves were determined from the frequency shift and quality factor ($q \sim 3 \times 10^4$) of dimensional acoustic resonance and also by the conventional pulse-echo method [10].

Laser irradiation was created by a focused 1.5-μ diameter beam or 1 × 4-mm band at wavelengths of 0.53 and 0.63 μm and a controlled intensity $I = 10^8$–10^{10} W/m^2. Refraction index measurements were performed by the compensation method [17].

3. RESULTS AND DISCUSSION

The original studies of induced effects concerned only the changes in the velocities of longitudinal and transverse acoustic waves depending on the total concentration of iron ions and the ratio $C_{Fe^{2+}}/C_{Fe^{3+}}$. It has been established that the average velocities of acoustic waves decrease with an increase in the total concentration of iron ions even without laser radiation and, conversely, the attenuation corresponding to them grows in proportion to C_{Fe} (Table 1, Fig. 2).

Scanning with a narrow acoustic beam (diameter, ~1.5 mm) over the cross sections of samples along the X and Z axis, the existence of elastic heterogeneities exhibiting as a change in the velocity $\delta V = \Delta V/V$ and the attenuation $\Delta\alpha/\alpha$ of acoustic waves in the initial

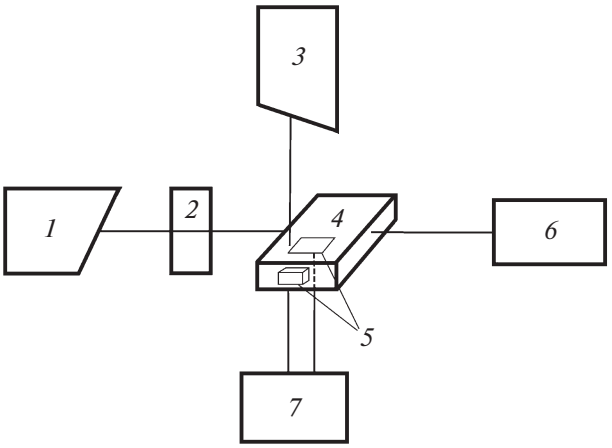

Fig. 1. Block structure of the setup for studying the effect of laser radiation on the elastic characteristics of lithium niobate samples: (*1*) laser, (*2*) collimator, (*3*) auxiliary laser, (*4*) lithium niobate sample, (*5*) electrode transducers, (*6*) module for the measurement of optic characteristics, and (*7*) generator of electromagnetic oscillations.

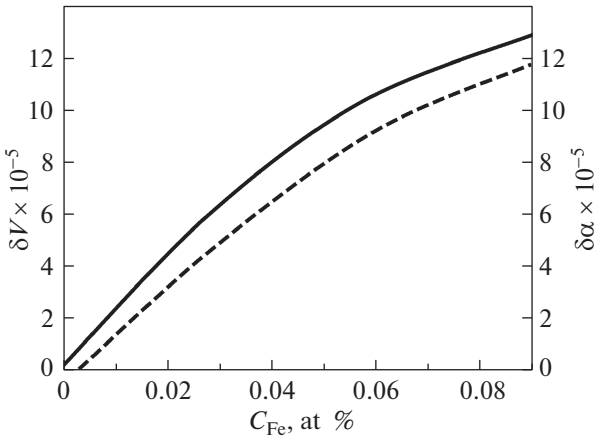

Fig. 2. Volume-average relative changes in velocities ($\delta V = (V - V_0)/V_0 = \Delta V/V_0$ (solid line) and attenuation $\delta\alpha = (\alpha - \alpha_0)/\alpha_0$ (dashed line) depending on the concentration of iron ions (C_{Fe}); V_0 and α_0 are the values at zero iron concentration before optic irradiation.

samples before thermal annealing and optical treatment was revealed. These local elastic heterogeneities correlate well with the changes in local refraction index values $|\delta n|$ (Fig. 3).

The above-mentioned acoustic and optic heterogeneities were partially smoothened after the annealing of samples under oxidative regime conditions at a decreasing ratio Fe^{2+}/Fe^{3+} to 0.1. Otherwise, annealing in the reductive regime at increasing Fe^{2+}/Fe^{3+} to 0.6 led to much greater acoustic and optic heterogeneities. In this case, the average acoustic and optic parameters remained nearly unchanged, and the observed deviations of the acoustic and optic parameter from their average values in the initial state abruptly grew.

When measuring the velocities of longitudinal and transverse acoustic waves under the laser radiation of $LiNbO_3$: Fe crystal X–Z section surfaces, it has been revealed that the photo-induced dependences of the velocity and the refraction index on the optical beam intensity in the samples subjected to reductive annealing correlate well with each other (Fig. 4) and quite satisfactorily correspond to the plot $\delta n(I)$ presented in [18]. Under radiation with $\lambda = 0.63$ μm, the values of $\Delta V/V$ were much lower than at $\lambda = 0.53$ μm. The velocity was revealed to increase under the conditions of radiation with the propagation of longitudinal waves along the Z axis and to slightly decrease, when they propagated along the Y axis.

A similarity between the changes in the ultrasonic wave velocities and the refraction index under optic radiation depending on the laser exposure time was also observed (Fig. 5), being in correlation with a similar change in E_{ph} and δn in $LiNbO_3$: Fe samples [18, 19] with a concentration of Fe^{2+} ions of ~ 0.05 at %. The time characteristics for the return of the resonance frequency and the refraction index to their initial values after radiation are nearly the same.

Similarly to the photo-induced changes in the refraction index, the changes in the velocity of ultrasonic waves were maximal in the samples subjected to reductive annealing, i.e., at a relative concentration of Fe^{2+} ions of ~20–30%. The greatest increase in the velocity V_e was observed near the local irradiation area closer to the negative pole of the spontaneous polarization vector $-\bar{C}$, and a decrease in velocity corresponded to the local area closer to the pole $+\bar{C}$ (Fig. 6).

The optical radiation of reduced samples also led to changes in the attenuation of ultrasonic waves. Using the scanning with a narrow ultrasonic beam along the Z axis, it has been established that the greatest decrease in attenuation occurs in the optical irradiation region closer to the negative pole and, conversely, an increase in acoustic attenuation is observed at the positive pole of the polarization axis (Fig. 6).

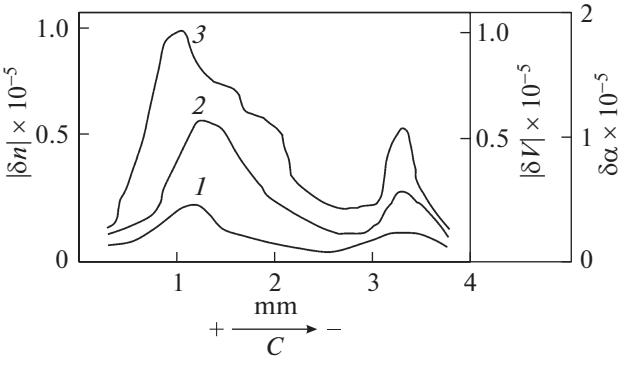

Fig. 3. Distribution of changes in (*1*) acoustic attenuation, (*2*) velocity, and (*3*) refraction index over the YZ cross section of sample no. 5a in the initial state.

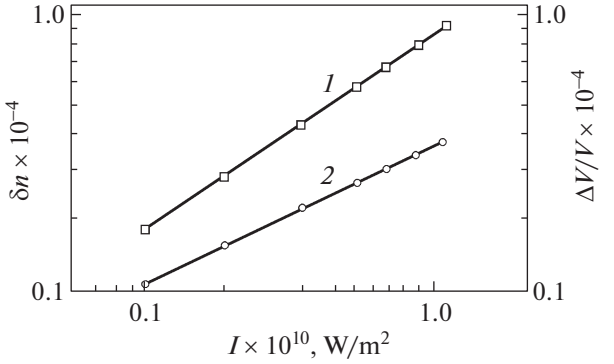

Fig. 4. Characteristics of change in (*1*) refraction index δn and (*2*) velocity $\Delta V/V_0$ under laser irradiation with $\lambda = 0.53$ μm and an increasing intensity with the propagation of a longitudinal wave along the *Z* axis.

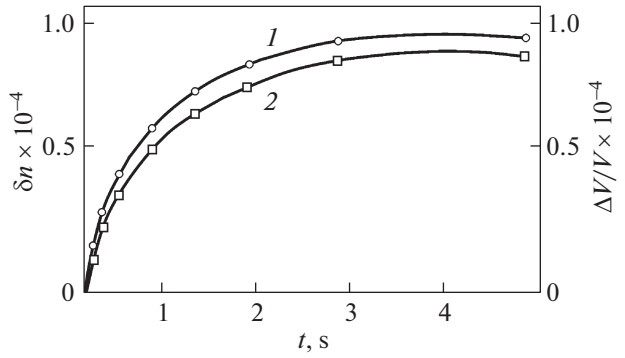

Fig. 5. Changes in (*1*) refraction index δn and (*2*) velocity $\Delta V/V_0$ depending on the irradiation time.

The maximum changes in the velocities of longitudinal and transverse acoustic waves at the greatest total concentration of iron ions and a Fe^{2+}/Fe^{3+} ion ratio optimal for the photorefractive effect (PRE) (Table 1) were used to determine the changes in the elastic mod-

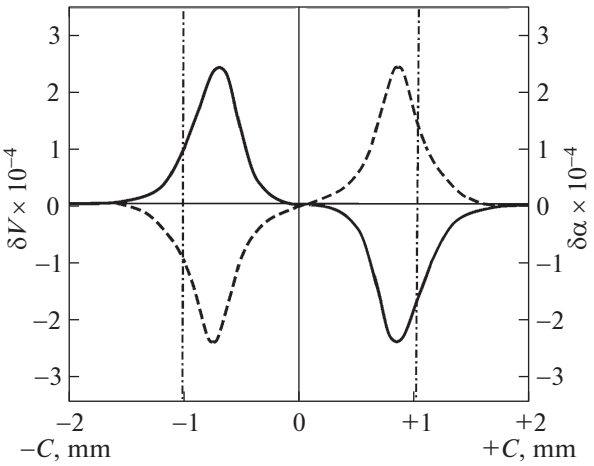

Fig. 6. Distribution of relative change in velocity δV (solid line) and attenuation $\delta\alpha$ (dashed line) along spontaneous polarization axis C. Dashed line is the laser irradiation area.

uli C_{33} and $(C_{11} - C_{12})/2$ by the expression $C_{ij} = \rho V_{ij}^2$ (Table 2).

Using the changes in the elastic moduli C_{33} and $(C_{11} - C_{12})/2$ with respect to pure $LiNbO_3$ samples, the elastic strains ε were determined as

$$\varepsilon_{ij} = N\eta Q/\Delta C_{ij}, \quad (1)$$

where N is the number of JT-ions per unit volume, η is the electron–lattice interaction constant, and Q is the quadrupole moment (Table 2).

In this case, the electron–lattice interaction constants (η) were taken from the measurement of electron paramagnetic resonance (EPR) parameters in a similar $LiNbO_3 : Fe^{2+}$ crystal [20, 21]. As a result, it has turned out that the sings of longitudinal and transverse strains completely coincide with the signs of similar strains given in [22] on the basis of theoretical calculations. A cross-sectionally nonuniform increase in the attenuation of acoustic waves before laser irradiation in the samples can also be explained by a nonuniform distribution of Fe^{2+} ions over them. In this case, α_{JT} will be related, according to the contemporary notions [14], with the change in the elastic moduli ΔC_{ij} and the time τ of relaxation between the states of electrons tunneling through the barrier as

$$\alpha = \frac{1}{2} k \frac{\Delta C}{C} \frac{\omega\tau}{1 + \omega^2\tau^2}, \quad (2)$$

where $k = \omega/V_0$ is the wave vector, V_0 is the velocities of acoustic waves, and C_0 is the elasticity moduli in the absence of JT-ions in a studied material.

In our case, the attenuation $\Delta\alpha \sim 30$ dB/m was obtained using the experimentally determined JT-changes in the elastic moduli C_{ij} and the relaxation times $\tau \sim 10^{-9}$ s known from the literature.

The additional changes in elastic moduli and attenuation under the irradiation with a laser beam were further determined in a similar way. It has been established that $\Delta C_{ij}/C_{ij}^{(0)}$ and α change over the cross section of an irradiated surface in proportion to the change in the concentration of Fe^{2+} ions, namely, a local increase in the concentration of Fe^{2+} ions leads to a decrease in the elastic moduli and, consequently, to a considerable increase in the ratio $(C_{ij} - C_{ij}^{(0)})/C_{ij}^{(0)}$ and a growth in attenuation. Otherwise, a local decrease in the concentration of Fe^{2+} ions (closer to the negative pole of the spontaneous polarization C) leads to an increase in the elastic moduli C_{ij} and a decrease in $\Delta C_{ij}/C_{ij}^{(0)}$ and $\Delta\alpha$, as observed in our experiments (Table 3).

The changes determined by us for the elastic strains induced by an intense laser beam ($I \sim 10^{10}$ W/m^2) with

Table 2. Relative change in elastic moduli $\Delta C_{ij}/C_{ij}$ and relative strains ε_{ij} for sample no. 5a in comparison with the pure sample at known values of the electron–lattice interaction constant η

$\frac{\Delta(C_{11} - C_{12})}{C_{11}^0 - C_{12}^0}$	$\frac{\Delta C_{33}}{C_{33}^0}$	η [100], cm^{-1}	η [001], cm^{-1}	ε [100]	ε [001]
1.2×10^{-4}	0.18×10^{-4}	110	90	3×10^{-5}	8×10^{-5}

Table 3. Relative change in elastic moduli, photostrains ε_{ph}, and refraction index δn depending on the concentration distribution of Fe^{2+} ions along axis C of sample no. 5a after laser irradiation (Fig. 6)

$C_{Fe^{2+}}$, 10^{25} m^{-3}	$\frac{\Delta(C_{11} - C_{12})}{C_{11}^0 - C_{12}^0}$, 10^{-4}	$\frac{\Delta C_{33}}{C_{33}^0}$, 10^{-4}	ε_{ph} [100]	ε_{ph} [001]	δn
1.5	3.5	1.1	5×10^{-5}	1.5×10^{-4}	5×10^{-5}
3.1	6.1	4.2	11×10^{-4}	2×10^{-4}	8×10^{-5}
4.7	9.2	6.3	15×10^{-5}	4×10^{-4}	2×10^{-4}

a precision of up to 20–30% correlate with similar photostrain values given in the work [13].

4. MICROSCOPIC MECHANISM OF PHOTO-INDUCED ELASTIC EFFECTS ASSOCIATED WITH JT-IONS

The analysis of experimental results obtained by us for optic and elastic effects has shown a common character of the processes occurring under optic irradiation. Just the exchange of charges between admixture JT-ions under optic irradiation is a root cause of local changes in the elastic characteristics of photorefractive crystals. Moreover, the obtained experimental data give additional evidences for the existence of a nonfield PRE mechanism.

Hence, the crystals in the initial state before optic irradiation contained local defect structures, which were nonuniformly distributed over their volume. Depending on the character of thermal annealing (oxidative or reductive), their effect on the optic and acoustic characteristics either increased or decreased, and this occurred with the same sign for the optic and acoustic characteristics. Optic irradiation also led to correlated changes in the optic and acoustic parameters.

Since Fe^{3+} ions are weakly bonded to the lattice of a crystal, it is obvious that the attenuation and velocity of acoustic waves will change in the case of any process (thermal annealing or optic irradiation) leading to a change in the concentration of Fe^{2+} ions. This statement is also confirmed by the spatial shift of the acoustic attenuation maximum towards greater concentrations of Fe^{2+} ions under laser irradiation.

Hence, the defect sites responsible for the photo-induced acoustic and optic effects may be admixture Fe^{2+} ions substituting lithium ions in the crystal lattice. As is known [12, 20–22], Fe^{2+} ions are bonded to the lattice of a crystal by means of strong electron–photon interaction. On the one hand, this interaction leads to local distortions in the lattice of a crystal near a JT-ion. In the case of lithium niobate, a nearly twofold increase in the concentration of Fe^{2+} ions at the boundary of laser irradiation under slight polarization conditions leads to microscopic tensile strain along the Z axis and microscopic compression strain along the X and Y axes. Hence, it is possible to hypothesize that the dynamics and spatial variations of macrostructural strains are governed in both cases by local distortions induced in the oxygen octahedra surrounding JT-ions by electric fields. On the other hand, periodic lattice oscillations (e.g., during the propagation of an acoustic wave) create modulation in the crystal field. The orbital motion of electrons, which leads to an effect on the orbital motion of spins due to spin–orbital coupling, is destroyed. Since the frequency of ultrasonic oscillations ($\nu \geq 200$ MHz) is much lower than the resonance frequency of acoustic EPR, additional acoustic attenuation and dispersion may be due in this case to the nonresonance transfer of energy from the lattice to electron spins, i.e., this is so-called relaxation acoustic paramagnetic attenuation. It has already repeatedly been observed for Fe^{2+} ions in different dielectric matrices [22].

5. CONCLUSIONS

As a result of performed experiments, it has been established that admixture Fe^{2+} JT-ions have an effect on the elastic characteristics of lithium niobate single crystals, creating a decrease in the elastic moduli and an increase in the attenuation of acoustic waves even in the absence of any external effects, including laser irradiation. The laser irradiation of admixture lithium niobate crystals with iron creates the photo-induced spatial redistribution of the concentrations of Fe^{2+} and Fe^{3+} ions. This process leads to an additional decrease in the elastic moduli and an increase in the attenuation of acoustic waves in the appearing local areas with an increased concentration of Fe^{2+} ions, and elastic strains appear at the boundaries of irradiated areas.

To our opinion, a main cause of photo-induced elastic effects in iron-doped lithium niobate is the formation of Fe^{2+} ion electric field gradients correlated along the trigonal axis with the accompanying axial strain of oxygen octahedra containing Fe^{2+} JT-ions.

ACKNOWLEDGMENTS

This work was performed within research state task no. 2014/448 (project code no. 2874).

REFERENCES

1. T. R. Volk and M. Wohlecke, *Lithium Niobate: Defects, Photorefraction and Ferroelectric Switching* (Springer-Verlag, Berlin, 2008).
2. *Ferroelectric Crystals for Photonic Applications*, Ed. by P. Ferraro, S. Grilli, and P. De Natale (Springer-Verlag, Berlin, 2009).
3. V. Y. Shur, in *Handbook of Advanced Dielectric, Piezoelectric and Ferroelectric Materials: Synthesis, Properties and Applications*, Ed. by Z.-G. Ye (Woodhead, Cambridge, 2008), p. 622.
4. A. V. Golenishchev-Kutuzov, V. A. Golenishchev-Kutuzov, and R. I. Kalimullin, *Photon and Phonon Crystals: Formation and Application in Opto- and Acoustoelectronics* (Fizmatlit, Moscow, 2010) [in Russian].
5. V. Y. Shur, Ferroelectrics **399**, 97 (2010).
6. A. V. Golenishchev-Kutuzov, V. A. Golenishchev-Kutuzov, R. I. Kalimullin, G. D. Mardanov, and A. A. Potapov, Ferroelectrics **441**, 25 (2012).
7. A. I. Korobov and V. E. Lyamov, Sov. Phys. Solid State **17** (5), 932 (1975).
8. V. V. Lemanov, G. A. Smolenskii, and A. B. Sherman, Sov. Phys. Solid State **11** (3), 524 (1969).

9. Yu. V. Vladimirtsev and A. V. Golenishchev-Kutuzov, Sov. Phys. Solid State **22** (1), 125 (1980).
10. V. A. Golenishchev-Kutuzov, N. N. Glebova, S. A. Migachev, and Y. V. Vladimirzev, Ferroelectrics **64**, 209 (1985).
11. Li-jie and K. Dransfeld, Z. Phys. B: Condens. Matter **68**, 169 (1987).
12. W. Keune, S. K. Date, I. Dezsi, and U. Gonser, J. Appl. Phys. **46**, 3914 (1975).
13. M. Calamiotou, N. Chrysanthakopoulos, and G. Papaioannou, J. Appl. Phys. **102**, 083527 (2007).
14. V. V. Gudkov, I. B. Bersuker, I. V. Zhevstovskikh, Yu. V. Korostelin, and A. I. Landman, J. Phys.: Condens. Matter **23**, 115401 (2011).
15. V. Dierolf and C. Sandman, Appl. Phys. Lett. **84**, 3187 (2004).
16. K. Toyoura, M. Ohta, A. Nakamura, and K. Matsunaga, J. Appl. Phys. **118**, 064103 (2015).
17. A. V. Golenishchev-Kutuzov, V. A. Golenishchev-Kutuzov, R. I. Kalimullin, and A. A. Potapov, Phys. Solid State **53** (3), 518 (2011).
18. M. Simon, F. Jermann, and E. Kratzig, Opt. Mater. **4**, 286 (1995).
19. K. Kitamura, H. Hatano, S. Takekawa, D. Schutze, and M. Aono, Appl. Phys. Lett. **97**, 082903 (2010).
20. V. A. Golenishchev-Kutuzov, V. V. Samartsev, N. K. Solovarov, and B. M. Khabibullin, *Magnetic Quantum Acoustic* (Nauka, Moscow, 1977) [in Russian].
21. J. W. Tucker and V. W. Rampton, *Microwave Ultrasonics in Solid State Physics* (North-Holland, Amsterdam, 1972; Mir, Moscow, 1975). 453 s.
22. R. L. Melcher, *The Anomalous Elastic Properties of Materials Undergoing Cooperative Jahn–Teller Phase Transitions* (Academic, New York, 1975), p. 1.

Translated by E. Glushachenkova

SPELL: OK